Energy, Mines and Resources Canada | Énergie, Mines et Ressources Canada

CANMET

Canada Centre for Mineral and Energy Technology | Centre canadien de la technologie des minéraux et de l'énergie

THE USE OF A FLOW-THROUGH REAL-TIME METHOD TO DETERMINE RADON GAS EMANATION RATES FROM URANIUM ORE SAMPLES

J. BIGU AND J. KELLY

ELLIOT LAKE LABORATORY

NOVEMBER 1982

23 pp

MINERALS RESEARCH PROGRAM
MINING RESEARCH LABORATORIES
DIVISION REPORT MRP/MRL 82-124 (TR)

THE USE OF A FLOW-THROUGH REAL-TIME METHOD TO DETERMINE RADON GAS EMANATION RATES FROM URANIUM ORE SAMPLES

by

J. Bigu* and J. Kelly**

ABSTRACT

The testing of an experimental technique and apparatus for the determination of radon gas emanation rates from uranium ore samples is described. The technique uses real-time α-counting and a flow-through radon gas detection method thereby enabling dynamic behaviour to be investigated. Experimental results are compared with theoretical predictions. Good qualitative agreement is found between experimental and theoretical data. No reliable quantitative comparison can as yet be made because of lack of pertinent data including ore grade and some physical characteristics and properties of the sample.

---

* Research Scientist and Radiation Project Leader, Elliot Lake Laboratory, CANMET, Energy, Mines and Resources Canada, Elliot Lake, Ontario.
** Student, Waterloo University, on work term at Elliot Lake Laboratory, CANMET, Energy, Mines and Resources Canada, Elliot Lake, Ontario.

CONTENTS

	Page
ABSTRACT	i
INTRODUCTION	1
THEORETICAL BACKGROUND	2
Static Case	3
Dynamic Cases	5
EXPERIMENTAL APPARATUS	8
EXPERIMENTAL PROCEDURE	9
'Flushed' Experiment	9
'Non-Flushed' Experiment	9
EXPERIMENTAL RESULTS	10
DISCUSSION OF RESULTS AND CONCLUSIONS	13
CONCLUSIONS AND SUGGESTIONS FOR FURTHER WORK	19
ACKNOWLEDGEMENT	19
REFERENCES	20

FIGURES

No.		
1.	Diagram of experimental apparatus	4
2.	Theoretical ratio N_{Rn}/N_{Ra} versus radon gas build-up time for the static case (curve A), dynamic case A for $\lambda_v = 0.04$ min^{-1} (curve B) and dynamic case B for $\lambda_v = 0.04$, 0.1 and 0.2 min^{-1}, and S = 1, K = 1 (curve C)	6
3.	Alpha particle counts per min (cpm) versus elapsed time for flushed chamber experiment. Air flow rate is 0.3 L/min	11
4.	Alpha particle count per min (cpm) versus elapsed time for non-flushed experiment. The flow rate and radon gas build-up time were 0.21 L/min and 184 hours, respectively	12
5.	Integrated α-count versus radon gas build-up time. Alpha count integrated between zero and 150 min according to Fig. 4. All data obtained for a flow rate of 0.2 L/min except where indicated by arrows	14
6.	Alpha particle count per min, cpm, versus air flow rate	15

INTRODUCTION

Radon gas (Rn-222) and thoron gas (Rn-220) are decay products of the natural radioactive chains of U-238 and Th-232, respectively. Both minerals are widely and almost uniformly distributed in the Earth's crust. Usually both minerals are present in uranium ore samples, albeit in varying proportions, depending upon the chemical nature and origin of the sample. Radon and thoron due to their gaseous nature diffuse out of the uranium ore in which they are formed along fracture lines and porous openings in the rock. Once in the atmosphere, the short-lived decay products of radon and thoron may pose a health hazard if inhaled.

The rate at which radon and thoron escape from ore samples, henceforth called the emanation rate, is an important variable to consider when determining ventilation necessities in uranium mines to reduce radon daughter inhalation by occupational workers.

Emanation rates are usually determined by a static method whereby radon gas emanating from the sample, in an adequate container, is allowed to build-up for a period of time, and the activity of the gas in equilibrium with its decay products is measured by a suitable detector. Alpha activity and gamma activity methods have been used for determining radon gas emanation rates from rocks, soils and minerals (1-4 and references therein). The gas may or may not need to be transferred from the container holding the sample to the detector depending upon the radiation to be measured and the experimental apparatus used. In both cases referred to above, the α-activity and γ-activity measured can be related to the radon gas concentration produced during the radon gas build-up time, and hence the emanation rate.

This report describes a dynamic method for determining radon emanation

rates from uranium ore samples. This method differs from static methods in that it incorporates a detector of the flow-through type, thereby permitting real-time continuous monitoring of radon gas. Such a method has intrinsic advantages over static methods. Thus, the effect of temperature, barometric pressure, relative humidity and sample moisture content changes on the emanation rate can be studied in a continuous fashion. The method is particularly suitable for the study of transient phenomena. This report is a continuation of an on-going effort aimed at determining radon gas emanation rates (5).

THEORETICAL BACKGROUND

The emanation rate of radon gas is related to the emanation coefficient, whereby the latter is defined as the ratio of the radon released by the sample to the total radon formed within the sample. It is also defined as the fraction of radon produced in some mineral matrix which escapes the matrix and is free to diffuse in the pore spaces. The emanation coefficient of uranium ores ranges from about 0.01 to above 0.9, i.e., is usually less than unity as some radon is trapped irreversibly in the mineral structure. The emanation coefficient depends on a number of factors including the porosity, mineral species, radium mineralogy, particle size, interstitial or pore water content, barometric pressure and air flow.

The emanation rate and emanation coefficient is commonly determined by static methods (1 to 4) but they can also be determined in principle by dynamic methods such as the ones described here (also see reference 5).

In the 'static case' radon gas emanating from the sample is allowed to build up for a given period of time in the sample container. The radon gas is then transferred into an alpha particle or γ-radiation detector where activity is measured.

The 'dynamic case' differs in that an air carrier is passed through the sample container and the experimental system at a given constant flow rate. Air may be passed through the system after allowing radon gas to build up in the emanation chamber for a pre-established time, or it may be injected shortly after purging the emanation chamber to ensure that no radon build-up occurs until the moment the air is flowed through the system (see Fig. 1). The first and second methods will be referred to as the dynamic case with radon gas build-up and dynamic case without radon gas build-up, respectively. The static and dynamic cases will be briefly described below.

STATIC CASE

The rate of formation of radon gas from the decay of Ra-226 within a uranium ore sample can be described by the following expression:

$$\frac{dN_{Rn}}{dt} = N_{Ra}\,\lambda_{Ra} - N_{Rn}\,\lambda_{Rn} \qquad \text{Eq 1}$$

In the above Equation N_{Rn} and N_{Ra} are, respectively, the number of atoms of Rn-222 in the sample container and the number of atoms of Ra-226 in the sample. The radioactive decay constants for Rn-222 and Rn-226 are denoted by λ_{Rn} and λ_{Ra}, respectively.

The solution of Equation 1, subject to the initial condition $N_{Rn} = 0$ at $t = 0$ is:

$$N_{Rn}(t) = N_{Ra}(\lambda_{Ra}/\lambda_{Rn})\ (1-e^{-\lambda_{Rn}t}) \qquad \text{Eq 2}$$

where $N_{Rn}(t)$ represents the absolute number of Rn-222 atoms formed from Ra-226 for a build-up time t. However, as $N_{Rn}(t)$ is not the experimentally determined variable, but $N'_{Rn}(t)$, i.e., the actual number of Rn-222 atoms that escape the sample, the emanation coefficient, say K, can be defined as:

$$K = N'_{Rn}(t_{SB})/N_{Rn}(t_{SB}) \qquad \text{Eq 3}$$

where the subindex SB stands for static build-up and replaces t in Equation 2.

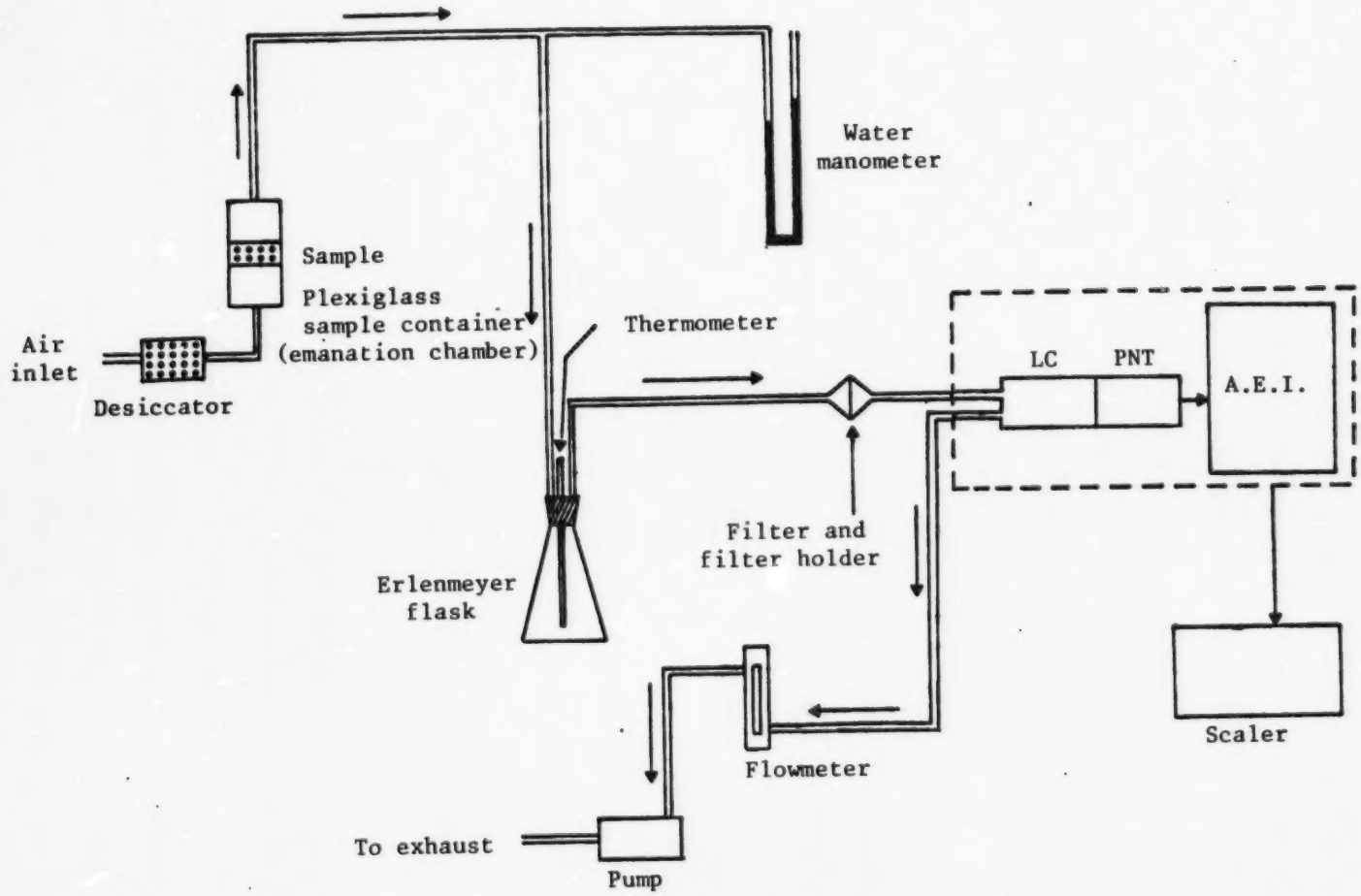

Fig. 1 - Diagram of experimental apparatus

Equations 2 and 3 can be used to determine K. The number of Rn-222 atoms that escape the sample, i.e., $N'_{Rn}(t_{SB})$ is given from Equations 2 and 3 as:

$$N'_{Rn}(t_{SB}) = \frac{K\, N_{Ra}\, \lambda_{Ra}}{\lambda_{Rn}} (1-e^{-\lambda_{Rn}\, t_{SB}}) \qquad \text{Eq 4}$$

The number of Ra-226 atoms in the sample, i.e., N_{Ra}, can be calculated from the ore grade of the sample by leaching methods. The condition $N_{Rn} = 0$ at $t = 0$ can be realized by flushing the container holding the sample thoroughly before the emanation experiment. This procedure is only acceptable for very high porosity samples. However, for medium and low porosity samples removal of Rn-222 from pores can be done under vacuum.

The build-up of Rn-222 from Ra-226 according to Equation 2 in a closed container is shown in Fig. 2A.

DYNAMIC CASES

A. Dynamic Case with Radon Gas Build-Up

For a flow-through method of the type discussed in this report a ventilation term must be added to account for the removal of radon from the emanation chamber, i.e., sample container, to the flow-through scintillation cell. The ventilation term is defined as $\lambda_v = \frac{Q}{V}$ where Q is the flow rate through the system and V is the volume of the sample container. Hence, the total removal of Rn-222 from the system is given by $\Lambda_n = \lambda_v + \lambda_{Rn}$ and Equation 1 becomes:

$$\frac{dN_{Rn}}{dt} = S - (\frac{Q}{V} + \lambda_{Rn})\, N_{Rn} = S - \Lambda_{Rn}\, N_{Rn} \qquad \text{Eq 4}$$

S in Equation 4 is a radon emanation factor which represents a steady supply of radon atoms per unit time from the sample (6,7). In this case $S = N_{Ra}\, \lambda_{Ra}$. Following a similar procedure as that used to derive Equation 2, the solution of Equation 4 is:

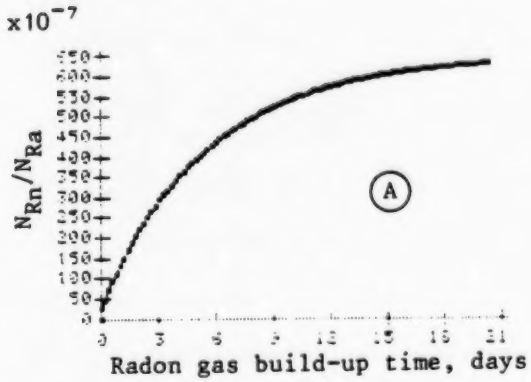

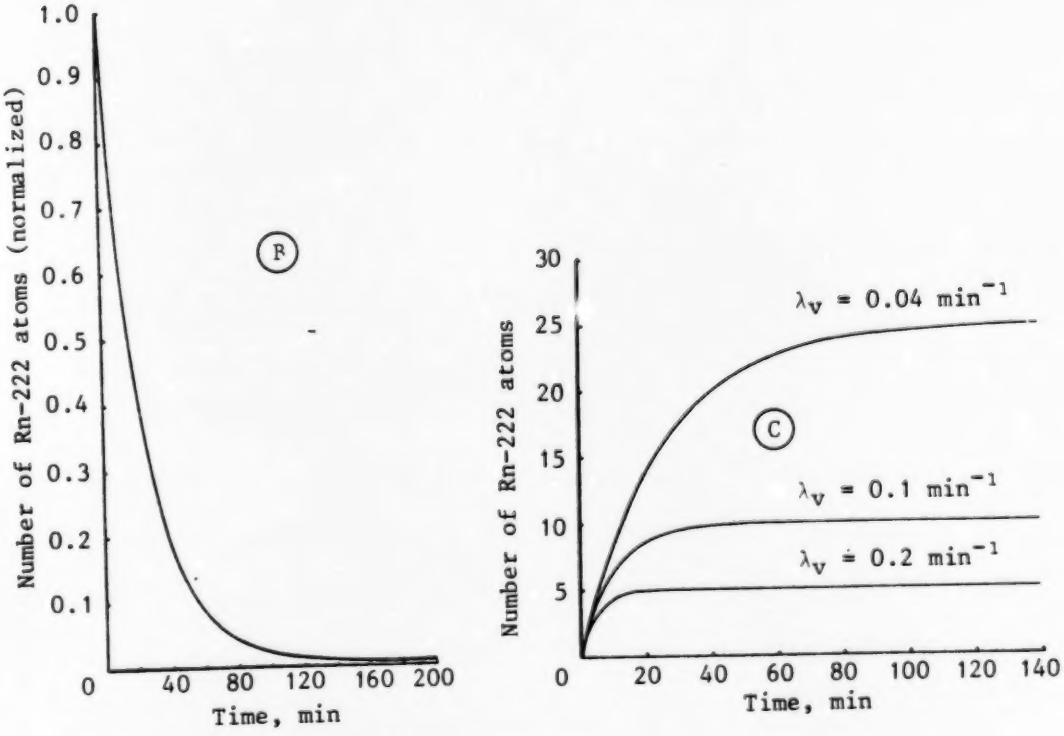

Fig. 2 - Theoretical ratio N_{Rn}/N_{Ra} versus radon gas build-up time for the static case (curve A), dynamic case A for $\lambda_v = 0.04$ min^{-1} (curve B) and dynamic case B for $\lambda_v = 0.04$, 0.1 and 0.2 min^{-1}, and S = 1, K = 1 (curve C).

$$N_{Rn}(t) = N_o\, e^{-\Lambda_{Rn}t} + \frac{S}{\Lambda_{Rn}}\,(1-e^{-\Lambda_{Rn}t}) \qquad \text{Eq 5}$$

where N_o represents the number of atoms of radon initially present at time zero, i.e., build-up concentration before passing air through the system and t is the time during which air flows into the system.

For an experiment in which Rn-222 is allowed to build-up with no air flow through the system, N_o is given by Equation 2. However, taking into account that not all Rn-222 emerges from the sample, Equation 4 should be used instead of Equation 2 and S should be substituted by an 'effective' or 'apparent' Ra-226 source strength given by SK. Hence, Equation 5 becomes:

$$N'_{Rn}(t) = KS\left[\frac{1}{\lambda_{Rn}}\,(1-e^{-\lambda_{Rn}tSB})\; e^{-\Lambda_{Rn}t} + \frac{1}{\Lambda_{Rn}}\,(1-e^{-\Lambda_{Rn}t})\right] \qquad \text{Eq 6}$$

where as before, $N'_{Rn}(t)$ represents the number of Rn-222 atoms diffusing out of the sample. Figure 2B shows the theoretical relationship between the number of atoms of Rn-222 and Ra-226 for K = 1, S = 1 and $\lambda_v = 0.04\ min^{-1}$, a value corresponding approximately to our experimental conditions, according to Equation 6. Notice that in Equation 6, $S = N_{Ra}\,\lambda_{Ra}$, as previously defined.

B. DYNAMIC CASE WITHOUT RADON GAS BUILD-UP

In this case a gas carrier is injected before any Rn-222 accumulation in the sample container. Hence, $N_o = 0$ and Equation 6 reduces to:

$$N'_{Rn}(t) = \frac{KS}{\Lambda_{Rn}}\,(1-e^{-\Lambda_{Rn}t}) \qquad \text{Eq 7}$$

Equation 7 shows that a steady-state is reached for large values of $\Lambda_{Rn}t$ when $e^{-\Lambda_{Rn}t}$ becomes much less than unity. Hence:

$$N'_{Rn}(t)_{SS} = \frac{KS}{\Lambda_{Rn}} \qquad \text{Eq 8}$$

where the subindex SS indicates steady-state. The same considerations as those indicated above apply to the second term of Equation 6.

It should be noted that Equations 4, 6, 7 and 8 are written in terms

of the number of Rn-222 atoms present. However, what is measured by an α-detector is the actual decay rate of these atoms, i.e., $A_{Rn}(=N_{Rn}\ \lambda_{Rn} = N_{\alpha})$ where N_{α} is the number of α-particles emitted by the decay of N_{Rn} per unit time, i.e., the α-count rate. Furthermore, as an α-detector is rarely 100% efficient, corrections have to be made for α-counting efficiency, ε. Writing $N_{\alpha,obs}$ and $N_{\alpha,true}$ for the observed and true α-count rate, respectively, one has the following relationship:

$$N_{\alpha,true} = N_{\alpha,obs.}/\varepsilon \qquad \text{Eq 9}$$

EXPERIMENTAL APPARATUS

A plexiglass cylinder (the emanation chamber), see Fig. 1, contains a uranium ore sample atop a sintered metal filter tray to allow an even distribution of a gas carrier (air). The cylinder is provided with inlet and outlet ports for air circulation. A desiccator column removes moisture from the air which then passes through the inlet port and through the plexiglass cylinder. Air carrying radon gas emanated from the sample passes into a 1,000 mL Erlenmeyer flask where local temperature may be measured. Following this, the air passes into the detection system after first passing through a filter (Millipore 0.8 μm) which removes all radon decay products in the gas sample.

The α-particle detection system consists of a scintillation cell (i.e., a cylindrical cell coated internally with a scintillator material, ZnS(Ag), and a transparent plexiglass window) optically coupled to a photomultiplier tube and associated electronic equipment, including a scaler where α-particle activity can be counted.

The cell is provided with inlet and outlet ports permitting continuous air flow by means of a sampling pump, and hence continuous α-activity determination. The volumetric air flow is measured by a calibrated air flowmeter

at the outlet port of the cell and the gas sampled is exhausted into the atmosphere. The system described in this report has been designed and used for similar types of measurements by Bigu (5).

EXPERIMENTAL PROCEDURE

Two different kinds of dynamic tests were conducted which will be referred to as the 'flushed' (i.e., Dynamic Case B) and the 'non-flushed' (i.e., Dynamic Case A) experiment.

'FLUSHED' EXPERIMENT

The operational procedure in this experiment was as follows. The scintillation cell and the emanation chamber with the ore sample were flushed independently with clean, filtered, air for about 15 min. The scintillation cell was flushed to eliminate all traces of radon gas. The emanation chamber was flushed at a high flow rate to eliminate undue build-up of radon gas and thus to initiate the experiment with essentially zero radon gas concentration. The end of the flushing period was recorded as time zero, the sampling pump was turned on and α-count rate as a function of time was noted. In addition, readings of barometric pressure, relative humidity and temperature were taken at regular intervals. At the end of the experiment the pump was shut off and the emanation chamber was isolated from the rest of the system by means of clamps placed at each end of its inlet and outlet ports.

'NON-FLUSHED' EXPERIMENT

In this case the emanation chamber was purged with a high flow rate sampling pump to remove all radon gas accumulated in it. Clamps were placed at the inlet and outlet ports of the emanation chamber and radon gas was allowed to build up for a predetermined period of time. The time of radon gas build-up was carefully noted, the clamps were removed at a given time, referred

to as zero time, and the sampling pump was turned on. The rest of the experiment proceeded as indicated for the 'flushed' experiment. However, because of radon gas build-up a transient phenomenon is observed when air flows through the system at a given flow rate at the beginning of the experiment, i.e., the α-count increases rapidly at the beginning, reaches a maximum and then decays slowly until a steady-state is reached (see Fig. 4). The transient portion of the alpha count versus time curve was integrated to obtain total α-count which was then related to the amount of radon gas in the container emanated during the build-up period.

EXPERIMENTAL RESULTS

Figure 3 shows the relationship of α-particle count rate in counts per min (cpm) versus elapsed time for an experiment of the dynamic type B where the sample container was flushed with air prior to the beginning of the experiment. Measurements were carried out with an air flow rate of 0.3 L/min. After a period of time (400 min), the supply of radon gas was removed, while still maintaining the same air flow rate through the cell, and the α-activity in the scintillation cell was recorded for some time to determine the remaining α-activity due to plate-out of radon daughter on the cell walls. Also indicated is the cell background before the beginning of the experiment.

Figure 4 shows the α-count rate (cpm) versus time for an experiment of the dynamic case A where build-up of radon gas in the container is allowed prior to the injection of air into the system at a flow rate of 0.2 L/min, approximately. Notice the transient behaviour exhibited in Fig. 4 for the α-activity. The area between the arrows indicates the region within which α-count was integrated in order to relate it to the amount of gas emanated during the build-up period, i.e., 184 h in this case.

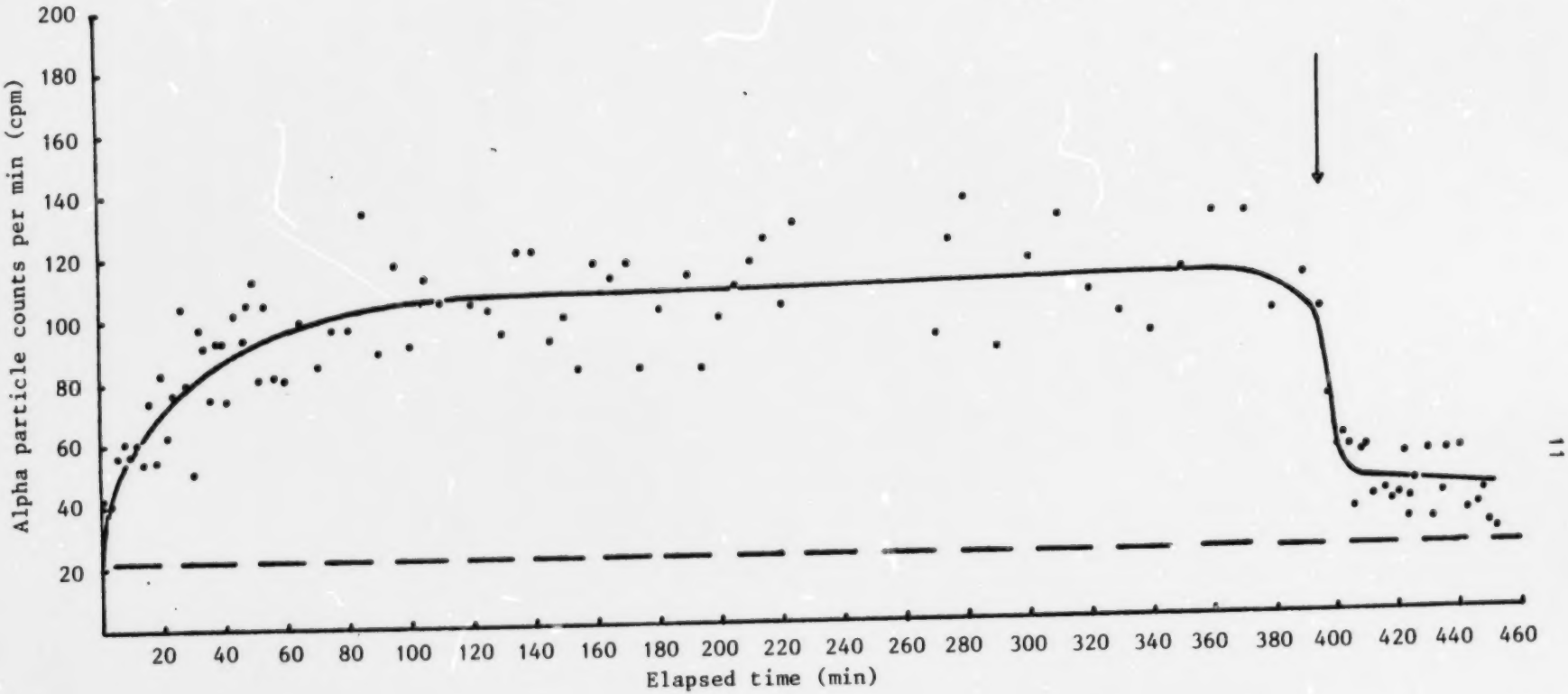

Fig. 3 - Alpha particle counts per min (cpm) versus elapsed time for flushed chamber experiment. Air flow rate is 0.3 L/min. The vertical arrow indicates removal of the radon source.

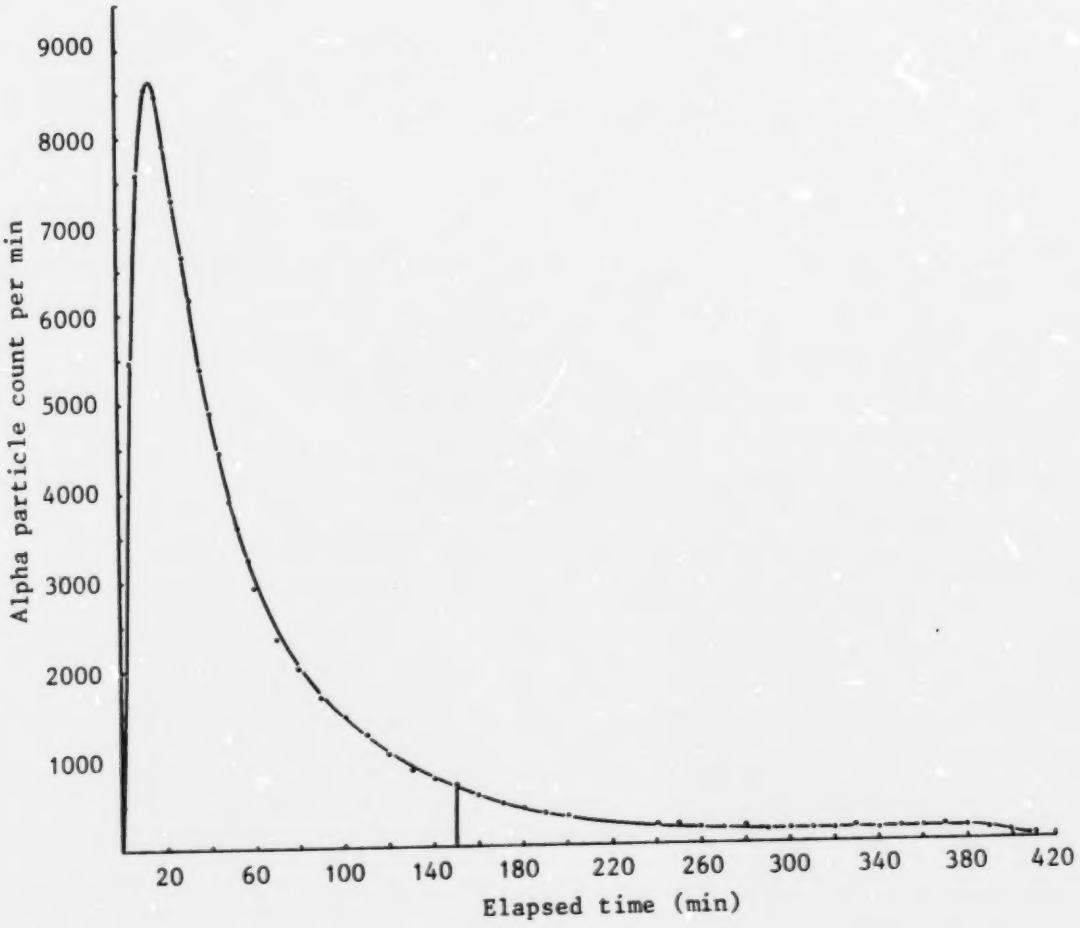

Fig. 4 - Alpha particle count per min (cpm) versus elapsed time for non-flushed experiment. The flow rate and radon gas build-up time were 0.21 L/min and 184 hours, respectively.

Figure 5 shows the integrated α-count obtained from Fig. 4 versus radon gas build-up time in days. A fixed α-count integration time of 150 min, starting at time zero, was used in all cases. Most experiments were conducted at an air flow rate of 0.2 L/min, but other flow rates were also used.

Figure 6 shows the α-particle count rate (cpm) versus air flow rate for a range of flow rates used in the present and other experiments not reported here.

DISCUSSION OF RESULTS AND CONCLUSIONS

Results obtained with the first procedure, (i.e., the flushed chamber experiment) correspond to the Dynamic Case B with no radon gas build-up. As stated in the procedure the emanation chamber was purged of all radon gas immediately prior to injection of air flow through the system and thus N_o was essentially zero. The graph of α-activity in cpm versus elapsed time (Fig. 3) obtained experimentally agrees well qualitatively with the theoretical predictions depicted in Fig. 2C corresponding to the ratio Rn-222/Rn-226 versus elapsed time (see Equation 5 with $N_o = 0$, or Equation 6 with $t_{SB} = 0$). In both graphs N_{Rn}/N_{Ra} (Fig. 2C) and N_α (Fig. 3) increase rapidly at the beginning to reach a plateau or steady-state value soon after. The time taken to reach this steady-state condition depends on λ_v. (Notice that Fig. 2C and 3 cannot be compared quantitatively but only qualitatively. The essential difference between these figures is a multiplier which includes λ_{Rn}, λ_{Ra}, S and K where the latter have been taken as unity for the theoretical calculations.) This behaviour is expected as the radon gas emanating from the sample reaches an equilibrium or steady-state when its rate of exhalation equals its rate of removal by the carrier gas, i.e., air.

The results obtained following the second experimental procedure, i.e.,

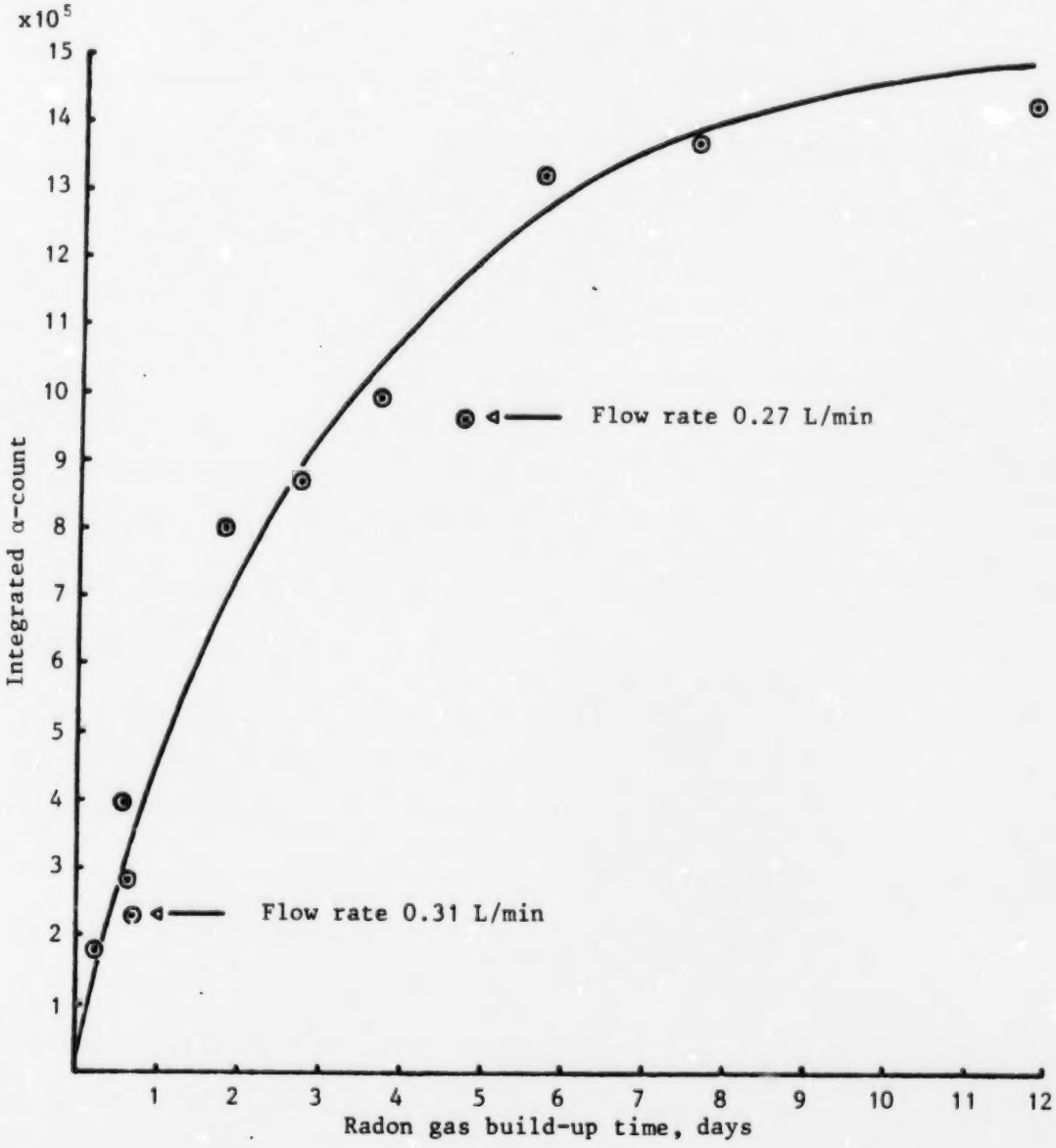

Fig. 5 - Integrated α-count versus radon gas build-up time. Alpha count integrated between zero and 150 min according to Fig. 4. All data obtained for a flow rate of 0.2 L/min except where indicated by arrows.

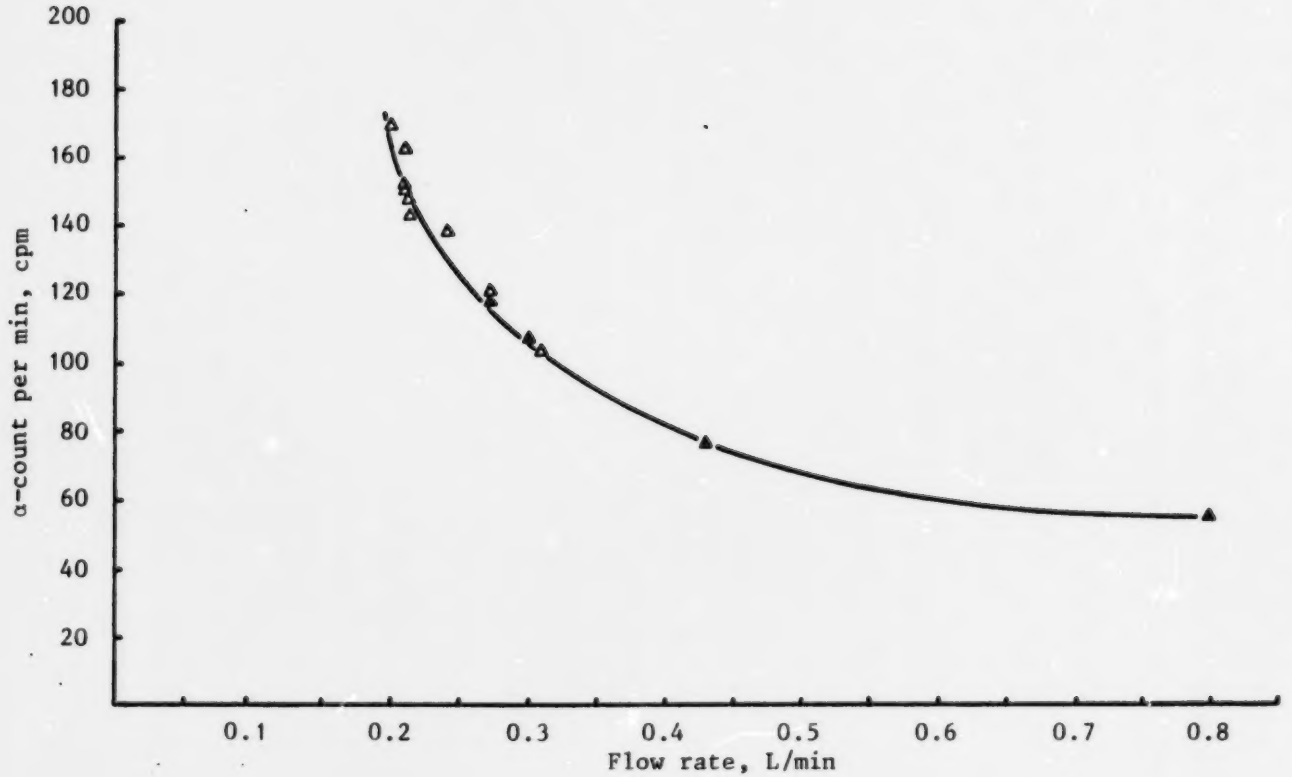

Fig. 6 - Alpha particle count per min, cpm, versus air flow rate.

non-flushed experiment where radon build-up is allowed (see Fig. 4), corresponds to the theoretical case depicted in Fig. 2B, i.e., Dynamic Case A with original radon gas build-up. Comparison of Fig. 2B and 4 shows only partial qualitative agreement in their dynamic behaviour. The α-activity profile shown in Fig. 4 is to be expected, however, as it reflects the complex dynamic nature of the process which results from the depletion of accumulated radon during the static build-up period, by air flow through the system, and subsequent detection of radon by the scintillation cell. Eventually, after the transient effect has subsided, the rate of removal of radon by the air flow equals the rate of radon exhalation by the sample and a plateau or steady-state condition is reached.

The main qualitative differences observed between Fig. 2B and 4 can be partly explained by noticing that Equations 5 and 6 give the N_{Rn}, and hence $A_{Rn} = N_{Rn} \lambda_{Rn}$, that would be detected by an appropriate detector (e.g., an α-scintillation cell) located immediately after the sample container, i.e., no physical separation, and hence no time delay, for radon to reach the detector. Furthermore, it is assumed (a) that the detector responds instantaneously to the incoming radon, and that the counting time can be made arbitrarily small, and (b) the radon gas concentration in the sample container is uniform and concentrated in a relatively small volume, i.e., small sample container. Also, the finite volume of the (flow-through) radon detector, and hence the radon gas transit time through it, about 1 min for Q = 0.2 L/min, is not considered. However, in actual practice, the following items should be noted:

1. The radon gas detector was located a distance of about 1 m apart from the sample container. In addition, as indicated above, an Erlenmeyer flask of about 1 L volume with temperature and differential pressure capabilities was installed in-line with the sample container and radon gas detector, the total volume, V, of the plastic tubing plus Erlenmeyer flask being about 1.2 L.

Taking into account that the experiments were carried out preferentially at a flow rate, Q, of approximately 0.2 L/min, the time delay, t, between gas emerging from the sample container and reaching the detector was about $t = V/Q = 1.2\ L/0.2\ L\ min^{-1} = 6\ min$.

2. The radon gas concentration in the sample container is not uniform as radon gas tends to concentrate at low points on account of its higher than air density, i.e., about 8 times more dense. Furthermore, some of the radon formed during the build-up period slowly diffuses through the sintered metal filter and into the lower section of the sample container, i.e., the buffer chamber. (Note: the total volume of the sample container is about 5 L, of which a volume of approximately 2 L forms the buffer chamber under the sintered metal filter.) A lower limit for the time taken by the sampling pump to displace the total volume of gas in the sample container can be calculated easily (see item 1). One obtains: $5\ L/0.2\ L\ min^{-1} = 25\ min$. In practice, however, this time could be considerably longer because the flow of air through the sample container is not likely to be uniform throughout its volume, thereby creating 'hot spots', i.e., locations where radon gas remains for long periods of time. This is particularly true for the buffer chamber below the sintered metal filter where radon gas is likely to be removed by the air flow at a much lower rate than that corresponding to the upper portion of the sample container. The above contentions are consistent with the 'tail', after the maximum, of Fig. 4. Eventually, a constant value for the radon concentration is attained which is again consistent with the values predicted by Equation 6 for large values of t for which the first term becomes vanishingly small and the second term reduces to the constant KS/Λ_{Rn}, i.e., long tail of Fig. 4.

3. Because of the higher, than air, density of radon gas (see item (2)), a layer

of undefined thickness towards the upper end of the sample container is pressumably composed of air only, or alternatively, there may be a relatively strong radon concentration gradient in the sample container, the concentration decreasing with increasing distance from the sample. This would have the effect of significantly decreasing the 'effective' volume of the sample container which in turn would (a) reduce the time to displace the radon gas in the container, and (b) increase the time taken for the radon gas to reach the detector. This is so because a decrease in the 'effective' volume of the sample container results in an increase in the 'empty' or 'dead' volume between the sample container and the radon detector. A compound effect is that due to the dilution of radon gas as soon as the sampling pump is operated. From the above discussion in item 3, it is reasonable to expect that the time taken for radon gas to reach the detector with $Q = 0.2$ L/min will be longer than the 6 min calculated in item 1, but less than the 25 min calculated in item 2. This is consistent with the peak at about 15 min experimentally observed (see Fig. 4).

Figure 5 shows that the total α-count obtained according to Fig. 4, i.e., integration between 0 and 150 min, is not linear and eventually reaches a maximum, constant value. This is to be expected as the radon gas concentration arising from the decay of Ra-226, increases until its rate of formation equals its rate of decay. The time at which this occurs depends upon the radioactive half-lives of Ra-226 and Rn-222 and can be predicted theoretically (see Equation 2 and Fig. 2A).

Experimental data pertaining to α-count rate versus sampling flow rate show that the former decreases with increasing flow rate in a predictable fashion as indicated by Equations 5 and 6. This behaviour applies to both dynamic cases studied here.

CONCLUSIONS AND SUGGESTIONS FOR FURTHER WORK

It may be concluded that the results obtained with the experimental apparatus and methods presented here agree well with the results predicted by theory. This applies to both types of dynamic experiments performed. However, it must be noted that this agreement is only of a qualitative nature because of the lack of some pertinent data such as the ore grade of the sample. Final results are forthcoming when radioanalyses of the sample are complete.

Major changes are being introduced in the apparatus described here based on the results obtained so far. Thus, in order to improve sensitivity and response time, the following modifications will be, or are being made:

a) Improved air injection system and/or operation under vacuum;

b) Modification of buffer chamber;

c) Reduction of sample container and incorporation into it of temperature and differential pressure monitoring capabilities; and

d) Because of item (c), elimination of Erlenmeyer flask and drastic reduction in plastic tubing length.

The methods and apparatus described in this report should prove useful to investigate dynamic situations of practical importance. Properly calibrated, the techniques described here should enable the determination of radon emanation coefficients from samples under a variety of static and dynamic conditions.

ACKNOWLEDGEMENT

The authors would like to thank M. Grenier for reading this manuscript, making useful comments and for some assistance in the experiments.

REFERENCES

1. Scott, J.H. and Dodd, P.H., "Gamma-only assaying for disequilibrium corrections"; RME-135, Geology and Mineralogy; April 1960.

2. Austin, S.R., "A laboratory study of radon emanation from domestic uranium ores"; in Radon in Uranium Mining, IAIA-PL-565/8, pp 151-163; 1975.

3. Barrettó, P.M.C., Clark, R.B. and Adams, J.A.S., "Physical characteristics of radon-222 emanation from rocks, soils and minerals: its relation to temperature and alpha dose"; in, The Natural Radiation Environment II, (Proc 2nd Int Symp Natural Radiation Environment, 1972), CONF-720805-P2, pp 731-740.

4. Austin, R.S. and Droullard, R.F., "Radon emanation from domestic uranium ores determined by modifications of the closed-can, gamma-only assay method"; Report of Investigation 8264; U.S. Bureau of Mines; 1978.

5. Bigu, J., "Design of an experimental system of the 'flow-through' type for laboratory measurements of radon gas emanation from uranium ores - a progress report"; Division ReportMRP/MRL 80-30 (TR); CANMET, Energy, Mines and Resources Canada; February 1980.

6. Beckman, R.T. and Holub, R.F., "Radon daughter growth with continuous radon influx and various ventilation rates"; Information Report 1099; U.S. Bureau of Mines; 1979.

7. Bigu, J., "Mine models and the thoron problem in underground uranium mines"; Proc Int Conf on Radiation Hazards in Mining: Control, Measurement and Medical Aspects; October 1981; Golden, Colorado; 1981; pp 243-255, Ed. Manuel Gomez, A.I.M.E., New York, 1981.